Hidden Intermediate State and Second Pathway Determining Folding and Unfolding Dynamics of GB1 Protein at Low Forces

Zilong Guo,[1] Haiyan Hong,[1] Guohua Yuan,[1] Hui Qian,[1] Bing Li,[2] Yi Cao,[2] Wei Wang,[2] Chen-Xu Wu,[1,*] and Hu Chen[1,†]

[1]*Research Institute for Biomimetics and Soft Matter, Fujian Provincial Key Lab for Soft Functional Materials Research, Department of Physics, Xiamen University, Xiamen 361005, China*

[2]*National Laboratory of Solid State Microstructure, Department of Physics, Collaborative Innovation Center of Advanced Microstructures, Nanjing University, Nanjing 210093, China*

(Received 14 January 2020; accepted 12 October 2020; published 6 November 2020)

Atomic force microscopy experiments found that GB1, a typical two-state model protein used for study of folding and unfolding dynamics, can sustain forces of more than 100 pN, but its response to low forces still remains unclear. Using ultrastable magnetic tweezers, we discovered that GB1 has an unexpected nonmonotonic force-dependent unfolding rate at 5–160 pN, from which a free energy landscape with two main barriers and a hidden intermediate state was constructed. A model combining two separate models by Dudko *et al.* with two pathways between the native state and this intermediate state is proposed to rebuild the unfolding dynamics over the full experimental force range. One candidate of this transient intermediate state is the theoretically proposed molten globule state with a loosely collapsed conformation, which might exist universally in the folding and unfolding processes of two-state proteins.

DOI: 10.1103/PhysRevLett.125.198101

When newly synthesized proteins emerge from ribosomes, they mostly fold to their native states [1] and must be unfolded before degradation by proteases [2]. The detailed mechanism of protein unfolding and folding remains one of the most challenging problems in the field of molecular biology [3].

During folding and unfolding transitions, most globular proteins adopt only two kinds of conformations: the native state (N) and the unfolded state (U). A simple two-state model which describes the folding dynamics of these proteins has been generally accepted [4]. Along a one-dimensional reaction coordinate, a transition state subject to a free energy barrier separates the N and U states. The properties of this transition state, including the height and position of the transition barriers, are crucial factors which determine the transition rates and the effect of the environment on the dynamics of protein folding and unfolding, and can be determined by well-designed experiments [5,6]. At the same time, it was reported that there might exist transient intermediate states between N and U states and we should consider that multiple pathways will give detectable effects on the dynamics of protein folding and unfolding [7,8].

The B1 immunoglobulin-binding domain of protein G from *streptococcus* (GB1) has been widely used as a model protein with which to study the mechanism of protein folding and unfolding. GB1 contains 56 residues, which form a globular structure with one α helix and four β strands [9]. Biochemical ensemble experiments with a stopped-flow quick mixing technique provides an opportunity to measure the dynamic process of protein folding and unfolding transitions with different concentrations of a denaturant [10].

Though GB1 does not sustain force in cells, it does show excellent mechanical properties due to its shearing characteristics of pulling geometry when force is applied to its N terminus and C terminus [11,12]. In forces ranging from 100 to 250 pN, it was found by atomic force microscopy (AFM) that the force-dependent unfolding rate $k_u(f)$ of GB1 follows Bell's model: $k_u(f) = k_u^0 \exp(f x_u / k_B T)$, where k_u^0 denotes the unfolding rate at zero force, x_u the unfolding distance, k_B the Boltzmann constant, and T the absolute temperature. The small x_u of 0.17 nm determined by AFM indicates that its unfolding transition state is very close to native state. Behavior of GB1 in artificial muscle [13] and hydrogel [14] is based only on measurements made at large forces. Whether $k_u(f)$ of Bell's model can be extrapolated to a low force regime remains unknown.

At force regimes < 30 pN, it was found that unfolding rates deviate from Bell's model for src SH3 protein by optical tweezers [15] and titin I27 protein by magnetic tweezers [16]. I27 even shows catch-bond behavior at forces smaller than 22 pN. Recently, catch-bond unfolding behavior of GB1 was found by Izadi *et al.* at forces below 10 pN using optical tweezers [17]. However, their results were obtained from a protein construct of GB1 flanked with PEG linkers. In the absence of PEG linker, GB1 gave inconsistent results with a much slower unfolding rate. Therefore, more detailed investigation on the mechanical response of GB1 to large-range forces is needed.

Magnetic tweezers are different from AFM and optical tweezers, and can apply intrinsic constant force over a large range and can measure protein dynamics on a timescale of several hours [18,19]. In this study, we measured force-dependent folding and unfolding rates over a force range from 3 to 160 pN using ultrastable magnetic tweezers. The force-dependent logarithmic unfolding rate shows different slopes at different force ranges, including the catch-bond behavior with a negative slope between 10 and 14 pN. This complex unfolding behavior indicates that there is a hidden intermediate state (I) between the N and U states and a free energy landscape with multiple barriers can be quantitatively constructed. We also obtained the critical force (8.2 pN) and the zero-force folding free energy ($\sim 11.9\, k_B T$) for GB1 from equilibrium folding and unfolding dynamics under constant forces.

Constant loading rate measurement.—In magnetic tweezers experiments, a protein construct AviTag(biotin)-$GB1_8$-SpyTag was linked between a SpyCatcher-coated coverslip and a *streptavidin*-coated paramagnetic bead [Fig. 1(a)] [20,25]. We first applied a constant loading rate of 1 pN/s to stretch the GB1 construct, in which sequential unfolding events of suddenly increased extension steps [Fig. 1(b)] were observed, with all eight GB1 repeats unfolded when the force increased to 90 pN. Then we decreased the force at a loading rate of -1 pN/s, driving GB1 to fold into its native state when the force dropped below 5 pN. Successful folding was confirmed by similar unfolding signals upon stretching with the same loading rate. Multiple force-ramp cycles on four different tethers produced the unfolding force distribution of GB1 at loading rates of 1 and 0.2 pN/s, respectively [Fig. 1(c)]. Thereby, the most probable unfolding forces were determined as ~70 pN for a rate of 1 pN/s and ~50 pN for 0.2 pN/s. Fitting the analytical formula of unfolding force distribution based on Bell's model [20,26] gives $x_u = 0.25 \pm 0.03$ nm, which is slightly larger than 0.17 nm obtained by AFM at forces greater than 100 pN [11].

Constant force measurement.—Constant force experiments give direct model-independent measurements of force-dependent dynamics. Figure 2(a) shows a typical measurement of the folding and unfolding dynamics of GB1 at constant forces obtained using magnetic tweezers. First, all the eight GB1 protein domains remained at their native state at 2 pN. The force was then increased abruptly to 60 pN, and the corresponding extension time course was recorded at this force value. Extension exhibited eight distinct jump steps of size ~15.1 nm (Fig. S11), each corresponding to an unfolding event of one GB1 domain. Then the force was decreased to 6 pN, and it was found that corresponding extension dropped suddenly with decreasing force due to the entropic collapse of the unfolded semi-flexible peptide. This was followed by a further shortening process caused by folding transition of GB1. The successful folding to the native state of GB1 can be verified by a subsequent pulling test using a larger force, such as 60 pN. Following similar procedures, experiments of force-dependent unfolding over a large force range from 10 to 160 pN (Figs. S4 and S5) and force-dependent folding from 3 to 6 pN (Fig. S6) were carried out.

Taking advantage of the stability of magnetic tweezers, it is worthwhile to measure the folding and unfolding dynamics of GB1 at equilibrium, which was found to exist at forces from 5.0 to 9.0 pN [20]. Figure 2(c) shows the equilibrium extension time course at 8.0 pN. At the beginning, all eight GB1 domains were unfolded by large force > 60 pN, then we dropped the applied force down to 8.0 pN and recorded the folding and unfolding dynamics for a duration of 4000 s. In this way, it is possible to obtain the histogram of extension [smoothed over a time window of 0.5 s in Fig. 2(c)], which shows nine peaks, corresponding to the nine conformations with zero to eight unfolded GB1 domains. In order to obtain the force-dependent folding and unfolding rate, it is necessary to convert dwell time between successive unfolding and folding steps to pseudounfolding and folding dwell time (Fig. S8) [19].

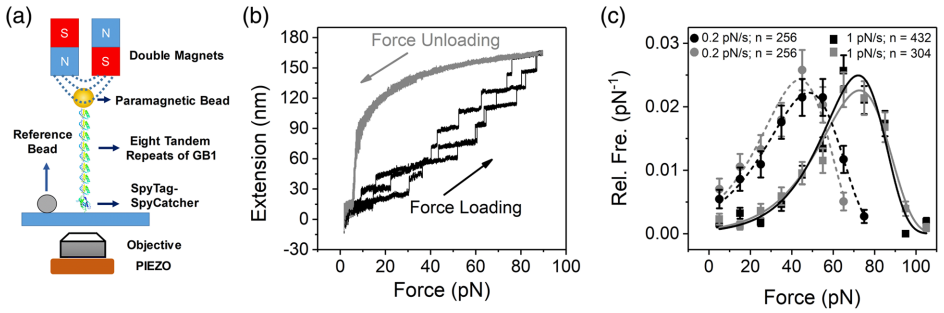

FIG. 1. Unfolding of $GB1_8$ in force-ramp experiments. (a) Sketch of magnetic tweezers with a protein construct $GB1_8$ linked between glass surface and paramagnetic bead. (b) Force-extension curve of $GB1_8$, measured in force-ramp experiments with constant loading and unloading rates of ± 1 pN/s. Each extension jump step corresponds to an unfolding event of a single GB1 domain. (c) Unfolding force distribution from four different tethers at constant loading rate of 0.2 pN/s (black and gray circles for two tethers) and 1 pN/s (black and gray squares for two tethers). Force distribution is fitted by prediction of Bell's model (Eq. S1) with $k_u^0 = (7 \pm 3) \times 10^{-4}$ s^{-1} and $x_u = 0.25 \pm 0.03$ nm [26]. Numbers of unfolding events are given in the legend.

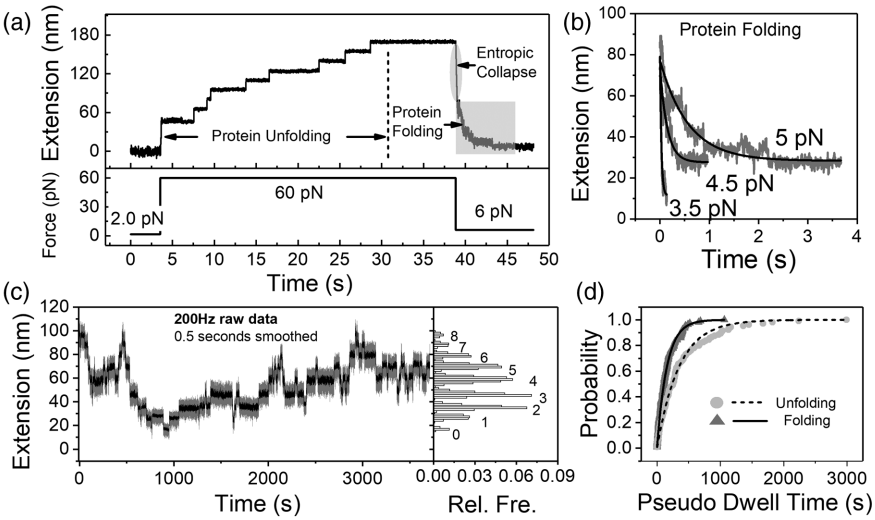

FIG. 2. Unfolding and refolding dynamics of $GB1_8$ at constant forces. (a) $GB1_8$ domains unfold in stepwise fashion after force increases from 2.0 to 60 pN. When force drops to 6 pN, entropic collapse of peptide (gray circle area) is followed by the folding process (gray square area). (b) Average folding time courses at 5.0, 4.5, and 3.5 pN from more than four folding time courses are fitted with exponential decay function to get $k_f(f)$. (c) Extension time course of 4000 s at 8.0 pN shows equilibrium folding and unfolding dynamics of $GB1_8$. Relative frequency of 0.5 s smoothed extension exhibits distribution peaks with zero to eight unfolded domains. (d) Unfolding and folding probability of GB1 was obtained by cumulative distribution of pseudo dwell time [19]. Dashed line and solid line show exponential fitting curves to determine k_u and k_f of GB1 at 8.0 pN, respectively.

Cumulative distribution of pseudounfolding and folding dwell time gives unfolding and folding probability as a function of time [Fig. 2(d)]. Exponential fitting gives unfolding and folding rates at each force level. These are shown as open symbols in Fig. 3.

From the folding and unfolding rates at the same force, the protein folding free energy at zero force can be calculated. For example, at 8.0 pN, folding free energy $\Delta G(f) = k_B T \ln k_f/k_u = 0.55\, k_B T$. Then the zero-force folding free energy is obtained as $12.1\, k_B T$ from Eq. S5. From equilibrium measurements at 7.0 and 9.0 pN, the corresponding zero-force protein folding free energies are $11.9\, k_B T$ and $11.7\, k_B T$, respectively. With the above equilibrium measurements, the average zero-force folding free energy is estimated as $\Delta G_0 = 11.9 \pm 0.2\, k_B T$, slightly larger than previous measurements with denaturant (7–$10\, k_B T$) [10,12,27]. We also estimated the critical force of GB1 as $f_c = 8.2$ pN, when $\Delta G(f_c) = 0$ and the folding rate and the unfolding rate are equal.

Figures 3(a) and 3(b) exhibit the unfolding rates and folding rates obtained from both equilibrium and force-jump measurements (mean value from at least three different tethers, Fig. S10). When the force is greater than 15 pN, Bell's model interprets well the force-dependent unfolding rate with $k_u^0 = 0.001\ \text{s}^{-1}$ and $x_u = 0.25$ nm, consistent with force-ramp measurements. Here, we noticed that the last two data points at forces of 140 and 160 pN give a smaller slope corresponding to $x_u = 0.13$ nm which is close to the result of AFM measurements at large forces [11,12].

When we enlarge the force-dependent unfolding rate, as shown in Fig. 3(b), the unfolding rates obtained by equilibrium measurement at 5–9 pN are approximately at the same level as the unfolding rates at 10–20 pN, but the logarithmic unfolding rate as a function of force shows a much bigger slope. Fitting with Bell's model at the force range of 5–9 pN gives $x_u = 1.0$ nm and $k_u^0 = 0.0004\ \text{s}^{-1}$. Consequently, the N-C distance of the native state, 2.65 nm plus x_u of 1.0 nm gives the size of unfolding transition state at a small force to be ~3.65 nm, much bigger than the transition state at forces > 15 pN. A surprising decrease in the unfolding rate is found from equilibrium measurement at 9 pN to nonequilibrium force jump measurement at 10 pN. In order to remove the suspicion that it is due to different measurement methods or different protein tethers, we did a force jump measurement on the same protein tether from 5 to 20 pN. Average results from five independent measurements show nonmonotonic force-dependent unfolding rates with catch-bond-like phenomenon in force range 10–14 pN, where the mean unfolding rate decreased from 0.0027 to $0.0019\ \text{s}^{-1}$ [Figs. 3(b), S9, S10(c)].

Compared with force-dependent unfolding, the folding rate is much more sensitive to force, decreasing by almost 5 orders of magnitude in the force range from 3 to 9 pN [Figs. 3(a), S10(d)] [28]. As folding starts from an extended peptide, the extension of unfolded peptide and the folding transition state can be used to calculate the force-dependent folding rate using Eq. S7. The measured force-extension curves of unfolded GB1 peptide can be described well by a wormlike chain model with a contour length of 21.7 ± 0.2 nm (~0.38 nm per residue) and a persistence length of 0.8 ± 0.1 nm (Fig. S11), which is consistent with

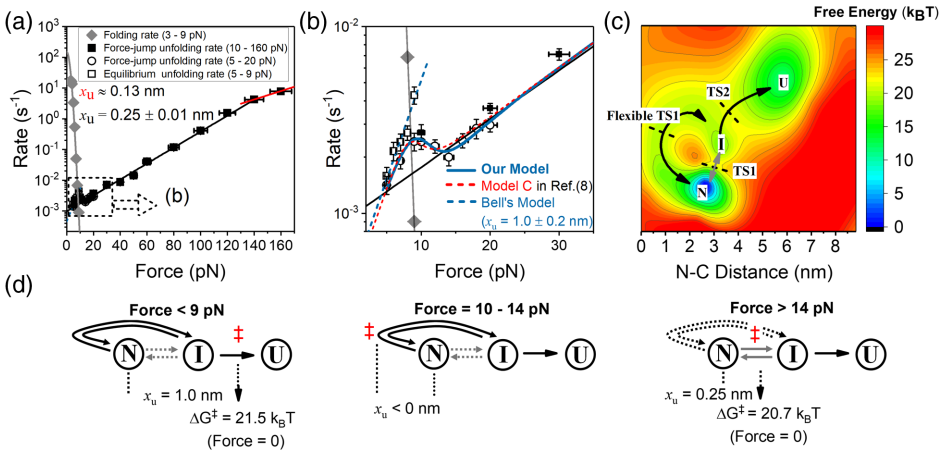

FIG. 3. Force-dependent folding and unfolding rates and two-pathway model for GB1 unfolding. (a) Folding rates and unfolding rates from force jump experiment and equilibrium measurement from 3 to 160 pN are summarized (Fig. S10). Slope determined by data points at 140 and 160 pN gives unfolding distance of ~0.13 nm (red line). Linear fitting in force range 15–140 pN determines $x_u = 0.25 \pm 0.01$ nm (black line), consistent with force-ramp experiment. Folding rate is fitted by Eq. S7 with folding transition state of size 3.65 nm and zero-force folding rate of $k_f^0 = 150 \pm 50\ s^{-1}$ (gray line). Error bar of folding and unfolding rates is given by standard error, and force is estimated to have 5% uncertainty. (b) Unfolding rates at 5–30 pN in (a) are enlarged. The unfolding rates in force range 5–9 pN obtained by equilibrium measurements are fitted with parameters $x_u = 1.0 \pm 0.2$ nm (blue dashed line). Nonmonotonic force-dependent unfolding rates at force-range 5–30 pN are fitted with a model with a hidden intermediate state and second catch-bond pathway (blue curve, Eq. S9). The dashed red line shows fitting result of model C in Ref [8] (Eq. S19), which is discussed in Supplemental Material [20]. (c) Diagram of a two-dimensional free energy landscape with three local minima (states N, I, U) and two unfolding pathways. Transition states are marked by dashed lines. (d) Model to explain the experimental results of $k_u(f)$. Solid arrows indicate the dominant pathway at different force range. The red double-dagger symbol represents the highest energy barrier position along the dominant unfolding pathway.

previous measurements of peptides at low forces [19,29]. Based on the measured force-extension curve of an unfolded peptide, force-dependent folding rate (Eq. S7) with $k_f^0 = 150\ s^{-1}$ and the size of folding transition state $l_{TS} = 3.65$ nm fits the experimental data well. Therefore, our result reveals a simple physical picture for GB1 that folding and unfolding transitions go through the same pathway and cross the same transition state.

Free energy landscape with two main barriers.—Unfolding distance at small forces below 9 pN is about four times as long as that at large forces, which clearly reveals that there is more than one barrier along the unfolding pathway. At forces larger than 15 pN, the relatively small unfolding distance x_u of 0.25 nm indicates that the conformation of the rate-limiting transition state (TS1) in this regime is very close to the native state of GB1. Based on previous MD simulations using experimental structural information, this transition state should be a structure with the three hydrogen bonds broken between the first and fourth β strands [30]. At small forces, the unfolding distance x_u of 1.0 nm proves a second unfolding transition state (TS2) with extension of ~3.65 nm, as shown in Fig. 3(c).

If we suppose the intrinsic conformation relaxation rate of a small protein is $\sim 10^6\ s^{-1}$ [31], the energy barriers can be estimated as 20.7 and 21.5 k_BT with the corresponding N-C distances of about 2.90 and 3.65 nm, respectively [Figs. 3(c) and S14]. As TS2 locates at an N-C distance ~0.75 nm longer than TS1, TS2 will have larger conformation changes in comparison with both N and TS1. Between TS1 and TS2, there must exist an intermediate state (I), a conclusion consistent with previous rapid mixing experiments which indicated a folding intermediate state for GB1 [32].

Kinetic model with intermediate state and two pathways.—If we suppose that there are two pathways between N and I, then a model with three states N, I, and U can be used to rebuild the complex force-dependent unfolding rate of GB1 [Fig. 3(d)] [33]. Equations and fitting parameters given in Supplemental Material [20] are consistent with values of x_u from previous fitting at different force ranges (Table S1 and Fig. S1). This model has not been proposed previously, and is a combination of two models discussed in [8]. At large forces, > 14 pN, GB1 unfolds through the pathway with positive x_u of 0.25 nm, and in this case barrier TS2 diminishes due its long apparent x_u of 1.0 nm. While at small forces < 9 pN, GB1 transits from N to I through the other pathway with an x_u of −2.4 nm, but it needs to cross a higher barrier TS2 so as to further unfold from I to U. At intermediate forces between 10 and 14 pN, the barrier in the pathway from N to I with negative x_u is higher than the second barrier TS2, which causes the catch-bond behavior of unfolding. The negative x_u of −2.4 nm

indicates that GB1 will collapse to very small extension in this pathway from N to I.

Catch-bond behavior at forces ranging between 10 and 14 pN can also be explained by a model which considers the possible flexibility of transition state TS1 (Fig. S14) [16,34,35]. The model does not contradict the above two-pathway model. In fact, the model with a flexible transition state can also be considered as a two-pathway model if the stretched transition state with longer extension and the collapsed transition state with shorter extension are treated as two different transition states.

Another model which can give similar nonmonotonic force-dependent unfolding rates was described in [8] [Fig. 3(b)]. With this model, however, the fitting results give ~4 nm extension difference between N and I states (Table S2), which indicates that the unfolding step size at large force should be ~4 nm shorter than the experimental results (Fig. S2), which excludes this model. This reminds us that the force-dependent unfolding rate alone cannot completely identify the free energy landscape which should also reproduce the experimental extension information.

Here, we think that this intermediate state [Figs. 3(c) and 3(d)] is simply the theoretically proposed molten globule state, which is composed of collapsed conformations with some nativelike secondary structures [36]. An intermediate state has been directly observed during the folding process of *E. coli* RNase H, a single domain protein with 155 residues, in an optical tweezers experiment [37]. At a force of ~5 pN, RNase H fluctuates between unfolded peptide and a globular intermediate state for several seconds before folding successfully to its native state. RnaseH is not, however, a typical two-state protein as it has a stable core which forms first during the folding process. A variant of RnaseH (I53D) shows two-state folding behavior without an intermediate state. Therefore, the intermediate state observed for wild type RnaseH is specific to this protein only. In contrast to RNase H, the intermediate state of GB1 between TS1 and TS2 cannot be directly recorded from the extension signal, indicating that it is a transient state with a very short lifetime.

In summary, using magnetic tweezers, we determined the force-dependent folding and unfolding dynamics of GB1 at a wide forces ranging from 3 to 160 pN. This has not been reported previously, either by AFM or optical tweezers alone. The equilibrium measurement directly determines the critical force of 8.2 pN and the zero-force folding free energy of GB1 $\sim 11.9\ k_BT$. Based on both the folding free energy and the complex nonmonotonic force-dependent unfolding rate of GB1 that is obtained, we constructed an energy landscape composed of a native state N, an unfolded state U, and a transient intermediate state I, which are separated by two barriers TS1 and TS2 whose location and barrier height are determined with TS1 very close to the native state and TS2 much longer than the native state. We proposed a kinetic model with two pathways between native state N and this transient intermediate state I, which is a combination of the two separate models discussed by Dudko *et al.* [8]. In this way, the complex force-dependent unfolding rates can be successfully rebuilt. The obligatory intermediate state is supposed to be the molten globule state and TS2 serves as a general barrier between compact molten globule state and the expanded unfolded state. Our results indicate that though the molten globule state is not as stable as the unfolded state and native state, it plays a universal role in protein folding and unfolding processes, even for single domain two-state proteins.

This research was supported by the National Nature Science Foundation of China (No. 11874309, No. 11474237, and No. 11574310 to H. C.) and the 111 Project (B16029).

*cxwu@xmu.edu.cn
†chenhu@xmu.edu.cn

[1] K. A. Dill and J. L. Maccallum, The protein-folding problem, 50 years on, Science **338**, 1042 (2012).
[2] M. E. Aubin-Tam, A. O. Olivares, R. T. Sauer, T. A. Baker, and M. J. Lang, Single-molecule protein unfolding and translocation by an ATP-fueled proteolytic machine, Cell **145**, 257 (2011).
[3] D. Thirumalai, Z. Liu, E. P. O'Brien, and G. Reddy, Protein folding: from theory to practice, Curr. Opin. Struct. Biol. **23**, 22 (2013).
[4] O. Flomenbom, J. Klafter, and A. Szabo, What can one learn from two-state single-molecule trajectories?, Biophys. J. **88**, 3780 (2005).
[5] J. C. Gebhardt, T. Bornschlogl, and M. Rief, Full distance-resolved folding energy landscape of one single protein molecule, Proc. Natl. Acad. Sci. U.S.A. **107**, 2013 (2010).
[6] O. K. Dudko, G. Hummer, and A. Szabo, Intrinsic Rates And Activation Free Energies From Single-Molecule Pulling Experiments, Phys. Rev. Lett. **96**, 108101 (2006).
[7] O. K. Dudko, Decoding the mechanical fingerprints of biomolecules, Q. Rev. Biophys. **49**, e3 (2016).
[8] C. A. Pierse and O. K. Dudko, Distinguishing Signatures of Multipathway Conformational Transitions, Phys. Rev. Lett. **118**, 088101 (2017).
[9] T. Gallagher, P. Alexander, P. Bryan, and G. L. Gilliland, Two crystal structures of the B1 immunoglobulin-binding domain of streptococcal protein G and comparison with NMR, Biochemistry **33**, 4721 (1994).
[10] E. L. McCallister, E. Alm, and D. Baker, Critical role of β-hairpin formation in protein G folding, Nat. Struct. Mol. Biol. **7**, 669 (2000).
[11] Y. Cao, C. Lam, M. Wang, and H. Li, Nonmechanical protein can have significant mechanical stability, Angew. Chem., Int. Ed. Engl. **45**, 642 (2006).
[12] Y. Cao and H. Li, How do chemical denaturants affect the mechanical folding and unfolding of proteins?, J. Mol. Biol. **375**, 316 (2008).

[13] S. Lv, D. M. Dudek, Y. Cao, M. M. Balamurali, J. Gosline, and H. Li, Designed biomaterials to mimic the mechanical properties of muscles, Nature (London) **465**, 69 (2010).
[14] J. Wu, P. Li, C. Dong, H. Jiang, B. Xue, X. Gao, M. Qin, W. Wang, B. Chen, and Y. Cao, Rationally designed synthetic protein hydrogels with predictable mechanical properties, Nat. Commun. **9**, 620 (2018).
[15] B. Jagannathan, P. J. Elms, C. Bustamante, and S. Marqusee, Direct observation of a force-induced switch in the anisotropic mechanical unfolding pathway of a protein, Proc. Natl. Acad. Sci. U.S.A. **109**, 17820 (2012).
[16] G. Yuan, S. Le, M. Yao, H. Qian, X. Zhou, J. Yan, and H. Chen, Elasticity of the transition state leading to an unexpected mechanical stabilization of titin immunoglobulin domains, Angew. Chem., Int. Ed. Engl. **129**, 5582 (2017).
[17] D. Izadi, Y. Chen, M. L. Whitmore, J. D. Slivka, K. Ching, L. J. Lapidus, and M. J. Comstock, Combined force ramp and equilibrium high-resolution investigations reveal multipath heterogeneous unfolding of protein G, J. Phys. Chem. B **122**, 11155 (2018).
[18] H. Chen, H. Fu, X. Zhu, P. Cong, F. Nakamura, and J. Yan, Improved high-force magnetic tweezers for stretching and refolding of proteins and short DNA, Biophys. J. **100**, 517 (2011).
[19] H. Chen, G. Yuan, R. S. Winardhi, M. Yao, I. Popa, J. M. Fernandez, and J. Yan, Dynamics of equilibrium folding and unfolding transitions of titin immunoglobulin domain under constant forces, J. Am. Chem. Soc. **137**, 3540 (2015).
[20] See Supplemental Material at http://link.aps.org/supplemental/10.1103/PhysRevLett.125.198101 for materials and methods, theoretical modeling, and supporting Figs. S1–S14, which includes Refs. [21–24].
[21] L. Li, J. O. Fierer, T. A. Rapoport, and M. Howarth, Structural analysis and optimization of the covalent association between spycatcher and a peptide tag, J. Mol. Biol. **426**, 309 (2014).
[22] Y. Cao, R. Kuske, and H. Li, Direct observation of Markovian behavior of the mechanical unfolding of individual proteins, Biophys. J. **95**, 782 (2008).
[23] M. Schlierf, H. Li, and J. M. Fernandez, The unfolding kinetics of ubiquitin captured with single-molecule force-clamp techniques, Proc. Natl. Acad. Sci. U.S.A. **101**, 7299 (2004).
[24] G. I. Bell, Models for the specific adhesion of cells to cells, Science **200**, 618 (1978).
[25] B. Zakeri, J. O. Fierer, E. Celik, E. C. Chittock, U. Schwarz-Linek, V. T. Moy, and M. Howarth, Peptide tag forming a rapid covalent bond to a protein, through engineering a bacterial adhesin, Proc. Natl. Acad. Sci. U.S.A. **109**, E690 (2012).
[26] G. Hummer and A. Szabo, Kinetics from nonequilibrium single-molecule pulling experiments, Biophys. J. **85**, 5 (2003).
[27] A. Morrone, R. Giri, R. D. Toofanny, C. Travaglini-Allocatelli, M. Brunori, V. Daggett, and S. Gianni, GB1 is not a two-state folder: Identification and characterization of an on-pathway intermediate, Biophys. J. **101**, 2053 (2011).
[28] O. K. Dudko, T. G. W. Graham, and R. B. Best, Locating the Barrier for Folding of Single Molecules under an External Force, Phys. Rev. Lett. **107**, 208301 (2011).
[29] M. Rief, J. Pascual, M. Saraste, and H. E. Gaub, Single molecule force spectroscopy of spectrin repeats: Low unfolding forces in helix bundles, J. Mol. Biol. **286**, 553 (1999).
[30] Y. D. Li, G. Lamour, J. Gsponer, P. Zheng, and H. Li, The molecular mechanism underlying mechanical anisotropy of the protein GB1, Biophys. J. **103**, 2361 (2012).
[31] R. B. Best and G. Hummer, Diffusive Model of Protein Folding Dynamics with Kramers Turnover in Rate, Phys. Rev. Lett. **96**, 228104 (2006).
[32] S.-H. Park, M. R. Shastry, and H. Roder, Folding dynamics of the B1 domain of protein *G* explored by ultrarapid mixing, Nat. Struct. Mol. Biol. **6**, 943 (1999).
[33] A. Garai, Y. Zhang, and O. K. Dudko, Conformational dynamics through an intermediate, J. Chem. Phys. **140**, 135101 (2014).
[34] S. Guo, Q. Tang, M. Yao, H. You, S. Le, H. Chen, and J. Yan, Structural–elastic determination of the force-dependent transition rate of biomolecules, Chem. Sci. **9**, 5871 (2018).
[35] S. Guo, A. K. Efremov, and J. Yan, Understanding the catch-bond kinetics of biomolecules on a one-dimensional energy landscape, Commun. Chem. **2**, 30 (2019).
[36] R. L. Baldwin and G. D. Rose, Molten globules, entropy-driven conformational change and protein folding, Curr. Opin. Struct. Biol. **23**, 4 (2013).
[37] C. Cecconi, E. A. Shank, C. Bustamante, and S. Marqusee, Direct observation of the three-state folding of a single protein molecule, Science **309**, 2057 (2005).